BULLETIN OF THE EARTHQUAKE
RESEARCH INSTITUTE
UNIVERSITY OF TOKYO
Vol. 63 (1988) pp. 327-348

Low Seismicity, Low Coda-Q and Discontinuities of the Upper Crust in the Vicinity of the Iznik-Mekece Fault, the North Anatolian Fault Zone, Turkey

Tameshige TSUKUDA

Earthquake Research Institute, University of Tokyo

Kenji SATAKE, Yoshimori HONKURA

Faculty of Science, Tokyo Institute of Technology

S. Balamir ÜÇER and A. Mete IŞIKARA

Kandilli Observatory, Boğaziçi University, Turkey

(Received October 31, 1988)

Abstract

An attempt to detect microearthquakes was made in the Iznik-Mekece Fault region, a proposed seismic gap in the western part of the North Anatolian Fault Zone, during the period from July 6 to August 13, 1986. We set up six temporary stations installing very small vertical-component seismometers and portable analog event recorders equipped with either paper tapes or magnetic cassette-tapes.

A large number of earthquake events, 135 at most for one station, were registered, the majority of which were either distant earthquakes with S-P times over 15 sec or artificial explosions. Eight hypocenters were determined by using data from the three stations, and three more epicenters were estimated from data from two of the stations. All the epicenters are located outside of the central part of the seismic gap region. Only four microearthquakes, which cannot be located, were identified in the vicinity of the Iznik-Mekece Fault. The microseismic activity rate around our network is statistically estimated to be 23.0 events/year with a significance level of 10%.

Coda Q values are found to be very low, between 30 and 200, in the fault region at frequencies from 2 to 10 Hz compared with the values, between 70 and 300, of the surrounding region. Two possible explanations are proposed for this: scattering due to concentrated heterogeneous medium and temporal increase of intrinsic absorption related to preparation of a large earthquake.

The presence of a discontinuity at a depth of 8-9 km in the crust is suggested by interpreting predominant phases other than direct P and S waves on the seismograms, providing a possible key to understanding the complex features of the tectonic regime around the western edge of the North Anatolian Fault Zone.

1. Introduction

The space-time distribution of earthquake faulting along the North Anatolian Fault Zone, as pointed out by TOKSÖZ *et al.* (1979), suggests that the western portion of the fault zone from 29° to 30.5°E is a possible seismicity gap of the first kind as defined by MOGI (1980). The eastwest trending North Anatolian Fault branches off into two faults westward at

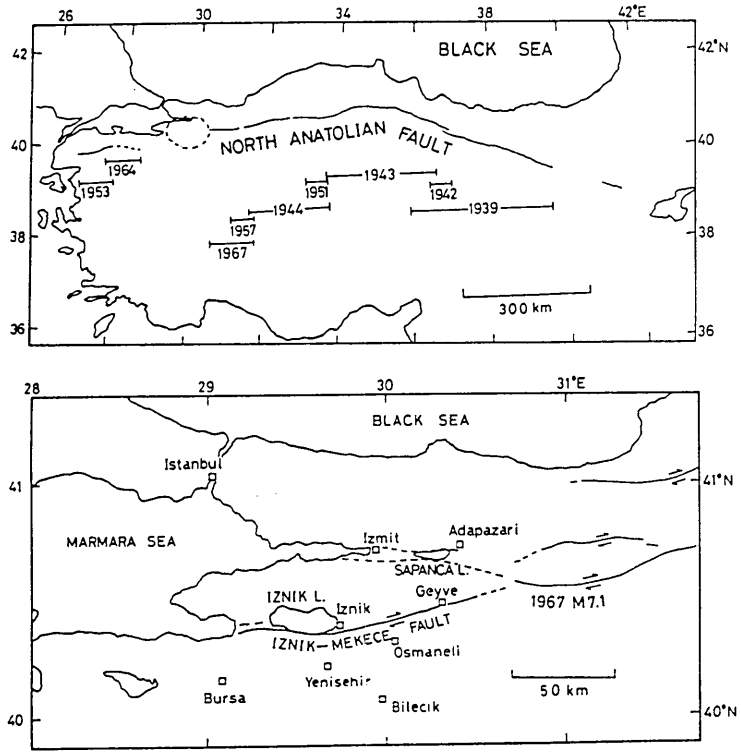

Fig. 1. *Upper*: Successive faulting with westward migration of large earthquakes along the North Anatolian Fault Zone (after AMBRASEYS, 1970). The 1939 Erzincan earthquake was the first break of the fault. The area enclosed by broken line is the seismic gap proposed by TOKSÖZ *et al.* (1979). *Lower*: Map around the seismic gap region. The traces of the Iznik-Mekece Fault and other active faults with clear topographic features are shown by solid lines; those with low clarity are drawn by broken lines (after IKEDA, 1988). A pair of arrows indicate strike slip movement of the fault.

around the source region of the 1967 Mudurnu earthquake of M7.1, which was the latest breakage in the westward successive migration sequence along the fault after the occurrence of the 1939 Erzincan earthquake of M8 (Fig. 1). A basin and range system separates the two branching faults. The northern branching fault or the Izmit-Sapanca Fault (IKEDA, 1988), is situated in a subsided zone running from east to west through the Sapanca Lake, Izmit Bay and Marmara Sea. The southern branching fault (SBF) or the Iznik-Mekece Fault (SIPAHIOĞLU and MATSUDA, 1986) passes through Iznik Lake in the next subsided zone. The two faults run nearly in parallel, about 30 km apart from each other.

The Izmit-Sapanca Fault is partly accompanied by remarkable microseismic activity, at least in the region close to Izmit City, which was revealed by a nearby temporary seismic observation (CRAMPIN *et al.*, 1985; EVANS *et al.*, 1985; LOWELL *et al.*, 1987). Small earthquakes of that region also have been recognized by data from MARNET, the routine telemetering observation network (ÜÇER *et al.*, 1985). On the other hand, the region around the Iznik-Mekece Fault has been quite aseismic even for small earthquakes with magnitudes around 3 or greater, as shown in Fig. 2. However, the low seismicity at a microseismic level has not been confirmed yet.

The purpose of this study is to estimate the degree of seismic activity

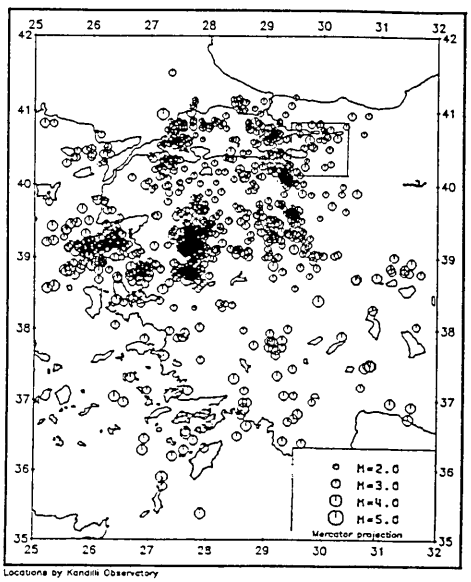

Fig. 2. Annual seismicity around western Turkey for 1985 obtained by Kandilli Observatory. The domain enclosed by a rectangle is the target region of our microseismic observations.

including microearthquakes in the vicinity of the Iznik-Mekece Fault in the middle of the proposed seismic gap and to find medium properties related to the fault. Our highly sensitive seismic observations from July 6 to August 13, 1986 were the first attempt to detect microearthquakes with magnitudes less than 2 in that fault region.

2. Observation Techniques

2.1. Instruments

We used two types of portable recording instrument. One was the STR-100 type event-recording system (Takamisawa Cybernetics Co. Ltd., Japan). Seismic wave data are initially stored on a 12 sec delay digital memory. When a signal with its amplitude beyond a prescribed threshold level is detected, a thermal printer-plotter will start to output waveform records on a 3 cm wide and 100 m long paper roll, printing also tiggering time and station identification number. The paper speed was set at 4 mm/sec, except at station ALA, where we adopted 8 mm/sec. Since the minimum amplitude we can read is about 0.5 mm and the maximum allowable one is 1 cm, the dynamic range of this system is 26 dB at the most. The record was set to be stopped 20 sec after the time when the amplitude decreased below the assigned threshold level.

Another type was a magnetic cassette tape event recorder developed by OIKE and MATSUMURA (1985). The principle of this instrument (OM-2) is as follows. Digitized seismic data are stored on RAM memory first, as similarly as in the STR-100. When a high amplitude signal is detected, the stored digital data will be transferred into an analog audio cassette tape recorder very quickly. By this process, the wave frequencies become 64 times higher than the original ones. This frequency modulation scheme produces compact seismic wave data on cassette tapes. One of the two channels of the cassette tape is used for two components of seismic signal, which are recorded in series separated by an 8 kHz beat signal. The other is used for time code signal from a quartz clock. In our case, one of the seismic components was replaced by a radio signal for absolute timing. The length of recording time on the cassette tape became about 4 sec in real time for each seismic event. We used casette tapes with a duration of 30 minutes, which allow about 400 events for each volume.

All the sensors were very small L-22D type vertical-component seismometers (products of Markproduct Co. Ltd, U. S. A.) with a natural frequency of 2 Hz. The sensitivity is 0.8 V/kine. The overall velocity frequency response of the total observation system is nearly flat in the range from 2 to 20 Hz for both STR-100 and OM-2 recording systems.

The timing of the quartz clock changed almost linearly, with a delay rate of 0.1-0.3 sec/day, since the atmospheric temperature varied only

slightly in summer. As a standard time we received a 15 MHz band radio broadcast from Moscow, U. S. S. R. When the radio wave was weak, as it often was in the evening, we adopted a wave of 10 MHz from Tashkent, U. S. S. R. For the STR-100, a radio signal was input in place of the seismic signal once every several days. Electric power was commercial alternating current. Quartz clocks, however, were backed up by batteries to work continuously even when the power supply interruped.

2.2. Observation Stations

Three STR-100 sets were installed in the central part of the target region, around the Iznik-Mekece Fault (See Table 1, Fig. 3). The distance between the stations is 20–30 km. This spanning is suitable for locating microearthquakes originating from the upper crust. Two of those three stations were located several kilometers off the fault in the villages of Alakaya in the west and Hacilar in the east. The other station was located near the town of Osmaneli, south of the fault.

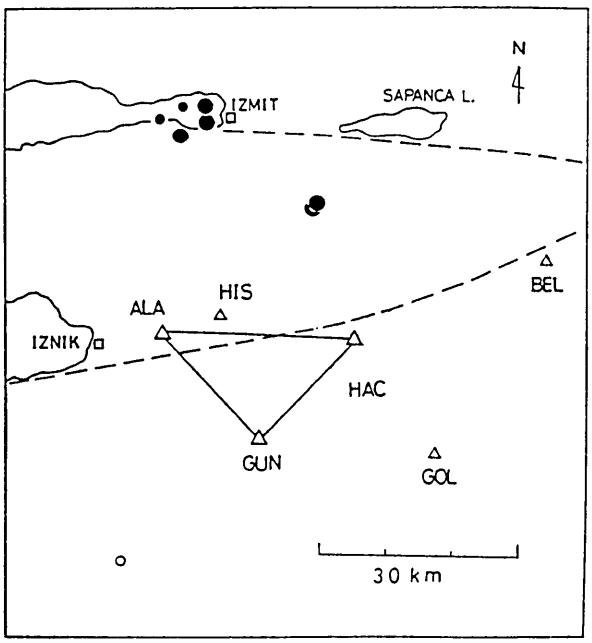

Fig. 3. Map showing seismic stations (open triangles) and epicenters determined by data from the three stations ALA, HAC and GUN. Large and small solid circles indicate earthquakes with magnitudes greater than and smaller than 2, respectively. Open circle denotes explosion. Broken lines denote fault traces: the Iznik-Mekece Fault (lower) and the Izmit-Sapanca Fault (upper).

Table 1. Locations of the microseismic temporary observation stations. The origin of the X-Y coordinate system is (30°E, 40.5°N). The uncertainty of location is 50-100 m in the horizontal directions.

CODE	NAME OF PLACE	LONGITUDE (°E)	LATITUDE (°N)	HEIGHT (m)	X (km)	Y (km)
ALA	Alakaya	29.8386	40.4395	630	−11.69	−6.70
HAC	Hacilar	30.1829	40.4416	640	15.52	−6.47
GUN	Günüören	29.9968	40.3041	380	−0.27	−21.75
HIS	Hisarcik	29.9211	40.4655	860	−6.69	−3.83
GOL	Gölpazari	30.3112	40.2877	595	26.46	−23.53
BEL	Belpinari	30.4906	40.5390	740	41.56	4.45

Alakaya station (ALA), the elementary school of the village, was on a hillside looking down the fault valley to the south. We installed the instruments in a lecture room, which was at our disposal since the school was on summer vacation. The transducer was put on the concrete floor in the room. The school building is located in the outskirts of the village and is founded on the bed rock. The ground noise level, therefore, is relatively small, the usual level ranging from 30 to 50 μ kine. However, peculiar impulsive signals, which apparently resemble the waveforms of ultra-microearthquakes having P and S pulses, were recorded very often at this station. After examination they were found to be noises produced by people banging doors of their houses.

The two stations HAC and GUN were also located at elementary schools. Since the basements of their buildings were not firm, resulting in large ground noise, we could not obtain as high gain as at Alakaya. Hacilar station (HAC), on the top of a hill several kilometers south of the fault, was situated on a fracture zone, which might be related to SBF. Günüören station (GUN) was located at the entrance of the village in front of a main path. The noise level was as high as 100-200 μ kine when traffic was high.

The above tripartite strations served as fundamental stations for monitoring the seismicity of the SBF and surrounding regions. Nearly continuous observations were kept for the three stations, as shown in Fig. 4.

In addition to the basic stations, we had three more stations where OM-2 recording systems were installed. The station in the village of Hisarcik (HIS) was located 10 km east of ALA. Belpinari station (BEL) was situated in the easternmost region, about 30 km east of the town of Geyve. The above two stations were also in elementary schools. But Gölpazari station (GOL) was located at a local forestry office, one of the permanent stations of Kandilli Observatory, Boğaziçi University.

The noise levels at the above three stations were so high that the cassette tapes had been often ran out before we exchanged them. BEL had particulary high ground noise level, because the residence of the

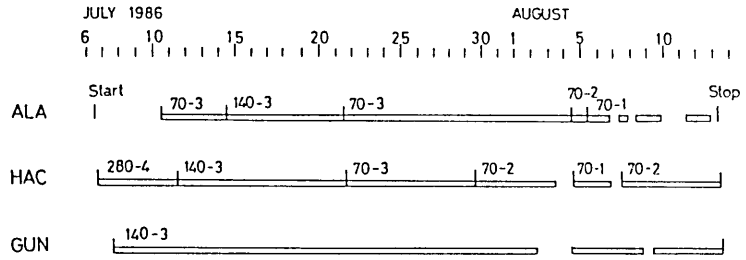

Fig. 4. Sensitivities and threshold levels for tripartite stations. The box shows the operation period. The numerals indicate the sensitivity in μ kine/mm (left) and the threshold level in the unit of sensitivity (right).

teacher's family was in the same building with the lecture room where the seismometer was set. At GOL the electric noise induced from a telephone line frequently disturbed input signal and, in effect, the frequency of triggering of the event recorder was enormously high, exceeding 100 times a day. Because of the above troubles we failed to obtain temporally homogeneous data at the stations equipped with the cassette tape recorders.

3. Microseismicity

The numbers of earthquake events were 75, 76, and 135 at ALA, HAC, and GUN, respectively, during 39 days. As shown in Fig. 5, the majority were distant earthquakes with *S-P* times over 15 sec, except for the data from GUN where many local artificial explosions were detected. Most of those regional events seem to come from the region around western Anatolia close to the Aegean Sea coast.

Local natural earthquakes with *S-P* times of less than 3 sec were quite small in number. At ALA, no seismic events were found for this *S-P* time range, in spite of the highest sensitivity of all three stations. For HAC and GUN, some events are probably not natural

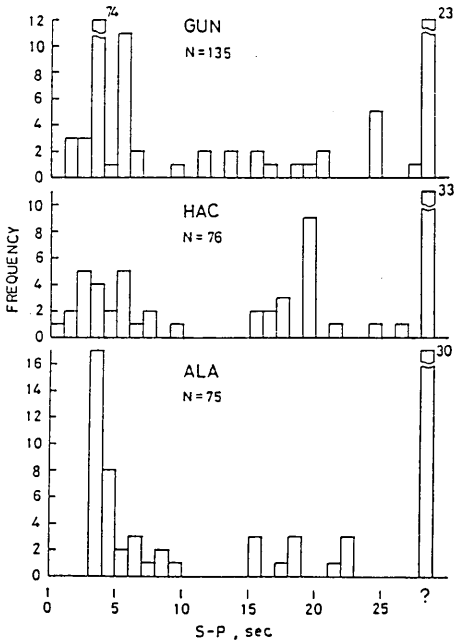

Fig. 5. S-P time distributions at the three stations (ALA, HAC and GUN). Teleseismc events whose S-P times are difficult to read are given at the right end (with ?).

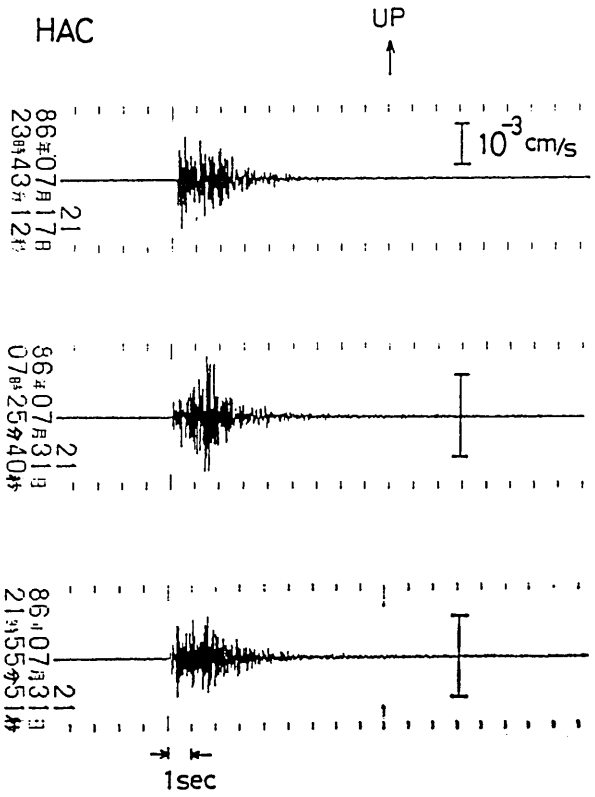

Fig. 6. Waveforms of ultra-microearthquakes recorded at HAC.

microearthquakes because their onset is not clear. Three and one local microearthquakes with S-P times of 2.2 sec or less were found at HAC and HIS, respectively; their sources may be located in the vicinity of the Iznik-Mekece Fault. Their seismograms are shown in Fig. 6 for HAC and in Fig. 10 (Event A) for HIS.

The peak around 3-4 sec in the S-P distribution at ALA represents the clustering activity near Izmit that had been observed already (ÜÇER *et al.*, 1985; EVANS *et al.*, 1985). During the observation period, 15 sequential clustering earthquakes were registered (Fig. 7). The largest event, of M2.8, was preceded by a bursting swarm including the second largest shock, of M2.2. Here we tentatively determined M (F-P magnitude) by the formula

$$M=-2.36+2.85\ \log(F-P), \qquad (1)$$

which is used for local earthquakes in the Kanto-Koshin'etsu network of the Earthquake Research Institute, University of Tokyo.

Most of the events with S-P times around 3-4 sec at GUN are esti-

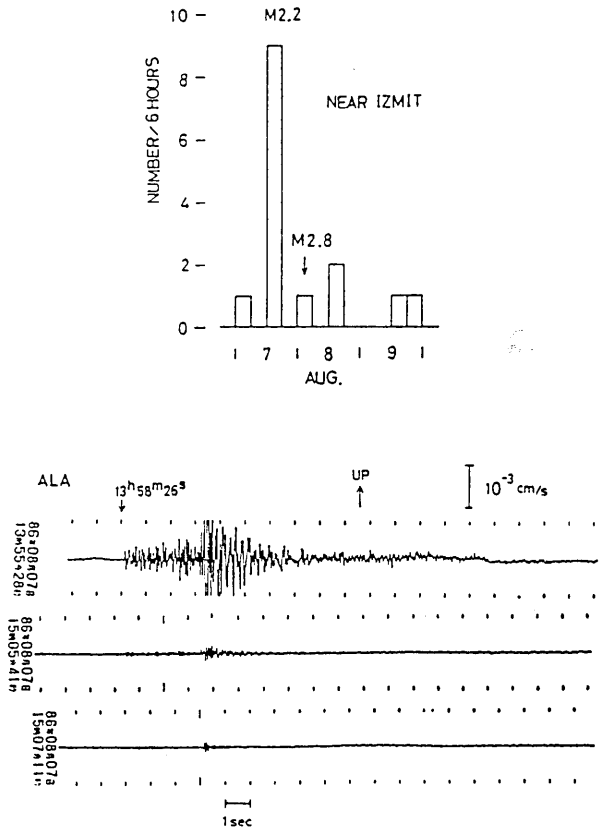

Fig. 7. Number of swarm earthquakes detected at ALA, for every 6 hours, and the waveforms recorded at ALA. The source area is around Izmit City.

mated to be explosions such as quarry blasts. Their peculiar waveforms with long-lasting coda waves as shown in Fig. 8 are indicative of shallow foci, and the occurrence local times were always in the daytime between 11 : 00 in the morning and 18 : 00 in the afternoon.

Eight local microearthquakes were recorded at all three stations with S-P times less than 5 sec. Furthermore, 14 shocks were recorded at two stations out of the three. As the crustal structure for the region concerned has not been studied in detail (CRAMPIN and ÜÇER, 1975), we assume here that the medium is a homogeneous half space with a P velocity of 6.0 km/s and a V_p/V_s ratio of 1.7, and determine hypocenters by a simple method. Origin times are obtained by using the linear relation between P time and S-P time (Wadachi Diagram). In the case of three stations, hypocenters are determined by finding the intersection of the three spherical surfaces whose radii are the corresponding travel distances

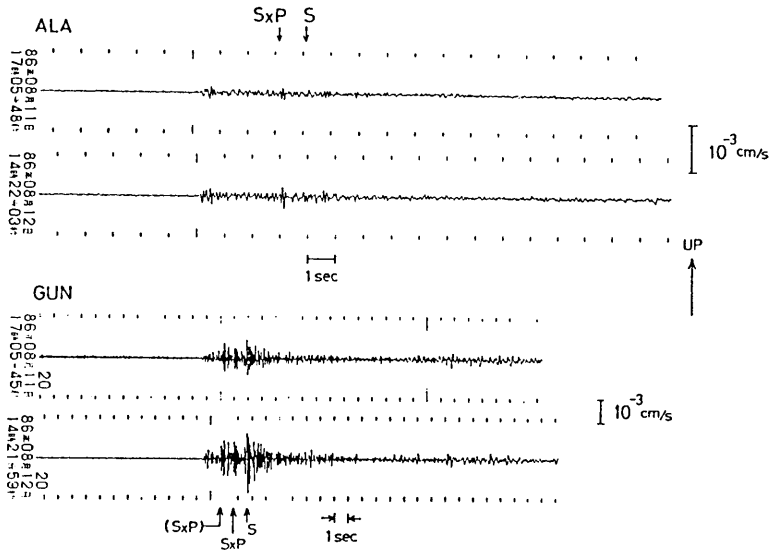

Fig. 8. Examples of waveforms of a series of explosions originating 30 km southwest of GUN. Two epicenters are determined as shown in Fig. 9(a).

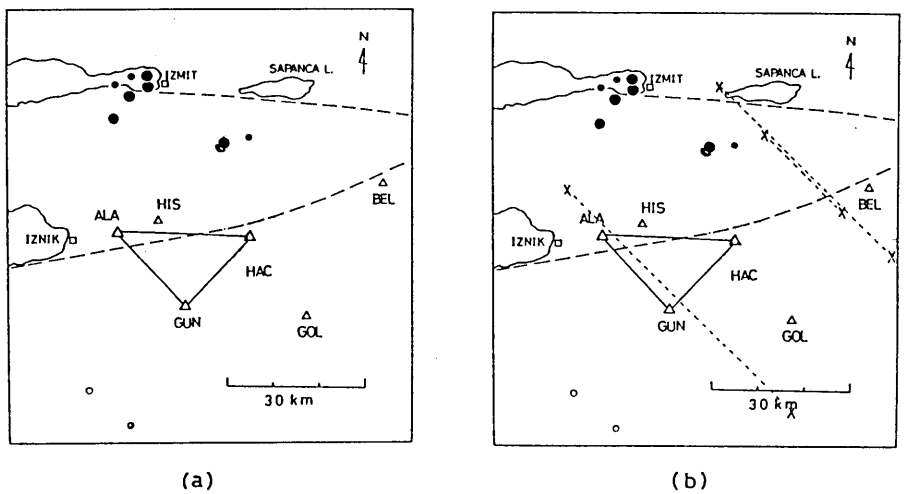

Fig. 9. Estimation of epicenters of shocks recorded at two of the three stations ALA, HAC and GUN. Solid and open circles indicate natural earthquakes and artificial explosions, respectively. Large ones are events with magnitudes greater than 2, and small ones less than 2. (a) Epicenters determined uniquely by the data from two stations as well as those given in Fig. 3. (b) Including all the data from only two stations. A pair of crosses linked with a dotted line shows the two possible epicentral solutions.

of P waves. In the case of two stations, we assume that the focus is on the ground surface, since, in our case, the hypocenters are so far away from the network that the depth cannot be accurately determined compared with the epicenter. After determining the origin time, all that is necessary is to find the intersection point of the two circles with the radii, the corresponding travel distances on the ground surface. In this case, we obtain two solutions in general. When its waveform resembles those of the events whose epicenters are located, we are able to select one solution from the two. For instance, the Izmit swarm earthquakes can be easily recognized when you look at the characteristic waveforms.

The epicentral distribution is shown in Fig. 3 in the case in which

Table 2. Hypocentral data for the events recorded at the three stations (ALA, HAC and GUN). The origin time is the local time. F-P times listed are from ALA. The last event is an explosion.

DATE	ORIGIN TIME h m s	X	Y (km)	Z	F-P (sec)	MAGNITUDE
Jul. 13	23 : 10 : 33.75	8.26	12.47	7.3	50	2.5
Jul. 14	00 : 36 : 30.90	8.26	12.47	7.3	50	2.5
Jul. 23	15 : 11 : 41.53	−8.18	27.28	13.3	45	2.4
Aug. 5	05 : 08 : 35.70	−7.95	25.06	13.0	25	1.6
Aug. 7	13 : 32 : 00.54	−11.87	22.78	7.0	45	2.4
Aug. 7	13 : 33 : 28.23	−11.75	22.20	17.3	20	1.3
Aug. 7	13 : 58 : 27.30	−14.92	25.42	16.7	20	1.3
Aug. 12	14 : 21 : 04.37	−19.41	−40.30	6.7	30	1.8

Table 3. List of local earthquakes recorded at two stations out of the three (ALA, HAC and GUN). The earthquakes are selected whose S-P times at one of the two stations are less than 6 sec. The origin time is the local time.

DATE	ORIGIN TIME h m	STATION	S-P TIME (sec)	F-P TIME (sec)	MAGNITUDE
Aug. 4	17 : 14	ALA	5.3	25	1.6
		GUN	3.6	20	1.3
Aug. 8	04 : 51	HAC	5.0	70	2.9
		GUN	5.5	70	2.9
Aug. 8	20 : 29	ALA	4.5	15	1.0
		HAC	2.8	15	1.0
Aug. 10	05 : 51	HAC	4.3	15	1.0
		GUN	6.3	13	0.8
Aug. 13	00 : 14	HAC	3.1	25	1.6
		GUN	5.5	22	1.5
Aug. 13	02 : 56	HAC	4.8	20	1.3
		GUN	4.3	18	1.2

data from all three stations are available. The results of the two station method are given in Fig. 9. Table 2 presents the hypocentral data. The focal depths range from 7 to 18 km. Table 3 shows the additional events located with seismic data from only two stations.

The region around the Iznik-Mekece Fault turned out to be very quiet in the recent microseismicity, the total number of shocks within 20 km from the stations being only four. Since the observation period was extremely limited compared with a long term period of more than several years, we must examine the above feature statistically based on a statistic model. If we assume that the time sequence of earthquake occurrence follows the Poisson random process, then the probability that we observe n or less earthquakes during the time interval T is

$$P=\sum_{k=0}^{n}\frac{(\mu T)^k}{k!}e^{-\mu T}, \tag{2}$$

where μ is the mean frequency of earthquakes. Let us make a statistical test assuming the significance level ε and estimate the mean frequency of microearthquakes based upon our observational result. The probability as a function of mean frequency should satisfy the relation

$$P<1-\varepsilon. \tag{3}$$

If we assume ε to be 0.1, the mean frequency is 23.0 events/year or less, provided that $n=4$ and $T=39$ days. The seismic level in the Iznik-Mekece region is such that we observe only 23 events in a year, with the probability of a false result being 10%.

4. Medium Properties beneath the Fault Region

4.1. Coda Q

We analyze coda waves appearing after the largest peak of S waves to study the attenuation of seismic waves in terms of Q values. Waveforms from local microearthquakes recorded on the cassette tapes were obtained at HIS, BEL and GOL. We performed A/D conversion of these waves at a sampling rate of 252 Hz. The reproduced waveforms are given in Fig. 10.

Following TSUKUDA (1988), we obtain the smoothed coda amplitudes u_{obs}, or running root-mean-square amplitudes for band-pass filtered waveforms against elapsed time t from the origin time of the shock. The time interval for running mean is taken as six times as large as the central period of the wave. Fig. 11 shows the modified smoothed amplitudes by

$$y_{obs}=\ln u_{obs}+\beta \ln t, \tag{4}$$

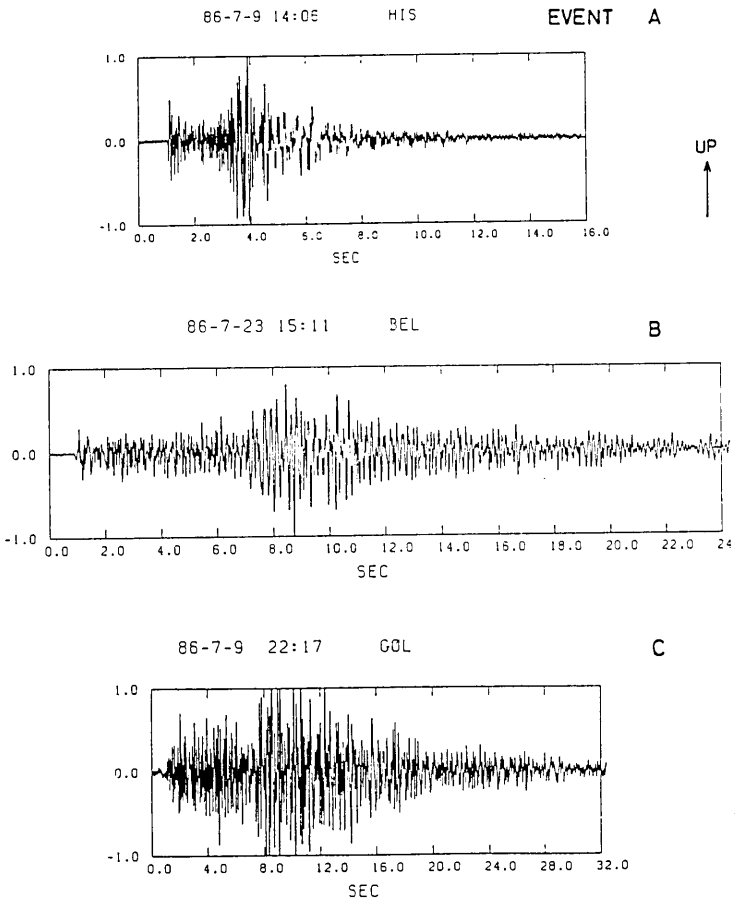

Fig. 10. Waveforms of local earthquakes recorded on the OM-2 cassette recorder. Amplitudes are normalized by the largest one for each event. Event A: The unique local earthquake with a small S–P time less than 5 sec recorded on this recorder. Event B: One of the clustering events near Izmit City. Event C: The earthquake that took place about 55 km east of GOL, judging from P and S times at GOL and GUN as well as the routine hypocentral data of MARNET at Kandilli Observatory.

where $\beta=1$ assuming body waves. The model function

$$y_{model}=const.-xfQ^{-1}t \qquad (5)$$

is fitted to the observed function (4) in the sense of least squares, where f is the central frequency.

Measuring errors of Q values are defined here to be the standard deviations of Q values calculated for different analysis intervals. The interval is changed by shifting one of the two end-points step by step until

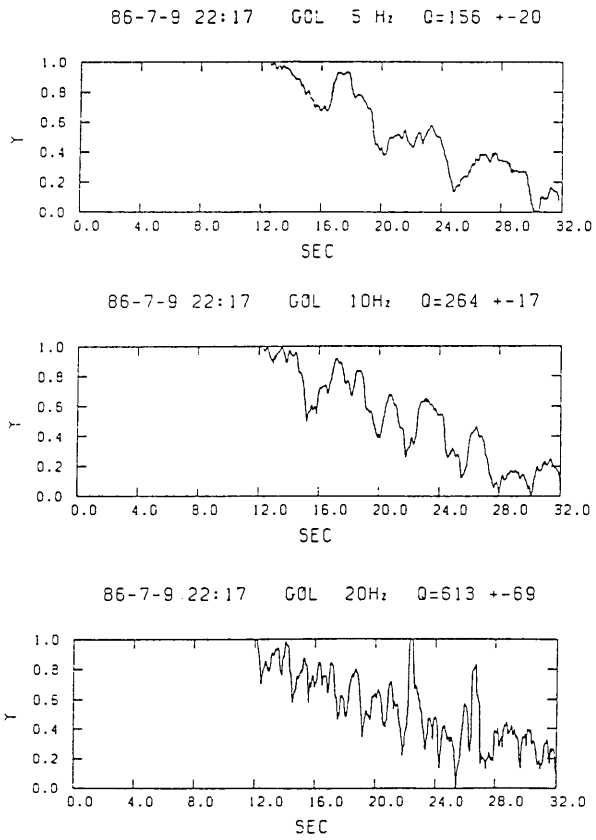

Fig. 11. Example of modified smoothed coda amplitude curves defined by equation (4) as a fuction of time for different frequency bands. The time axis is common with Fig. 10 (Event C). The amplitudes are normalized by the maximum.

its length is reduced to half of the entire length of analysis, and similarly for the other end-point.

The upper limit of the influence distances from which coda waves are generated is given by

$$r=(vt+d)/2\,, \tag{6}$$

where d, t and v are distance between epicenter and station, the upper limit of the travel times of coda waves analyzed and the S wave velocity, respectively. The values of r are 39 km from HIS, 97 km from BEL and 99 km from GOL, for Events A, B and C, respectively, provided that $v=$ 3.53 km/s.

The Q values obtained for different frequency bands show a systematic

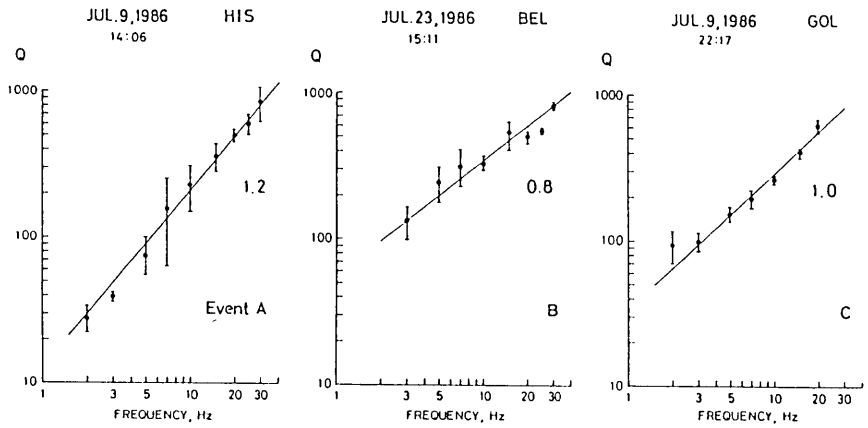

Fig. 12. Coda Q values as a function of frequency. Their frequency dependence is approximately expressed by $Q \propto f^r$, which is shown by straight lines. Numerals indicate the values of r. The error bars are obtained by taking the standard deviation of Q values calculated for 11 different time windows (See text).

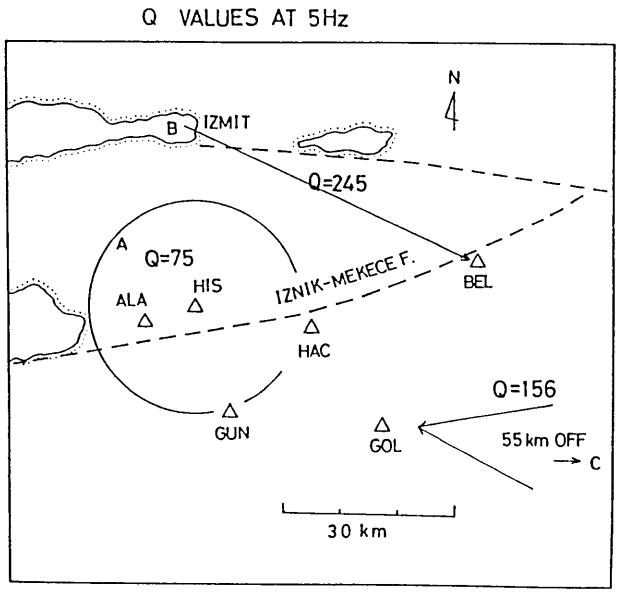

Fig. 13. Distribution of Q values at 5 Hz. The locations of sources of Events B and C are indicated by B and C, respectively. Event A took place within the circle centered at HIS.

dependence on frequency (Fig. 12). The Q values at lower frequencies, from 2 to 10 Hz, of Event A at HIS are anomalously low compared with other events with greater influence distances (Fig. 13). The slope r in

Fig. 12 for Event A is rather high compared with those of Events B and C and previous results obtained elsewhere (e. g. AKI, 1980 ; TSUKUDA, 1988), where r is measured as slightly less than 1. This low Q property may be due to either scattering by a concentrated heterogeneous medium around the fault with a correlation length of 350–1800 m or recently intensified intrinsic absorption when a large earthquake is being prepared as suggested by JIN and AKI (1986).

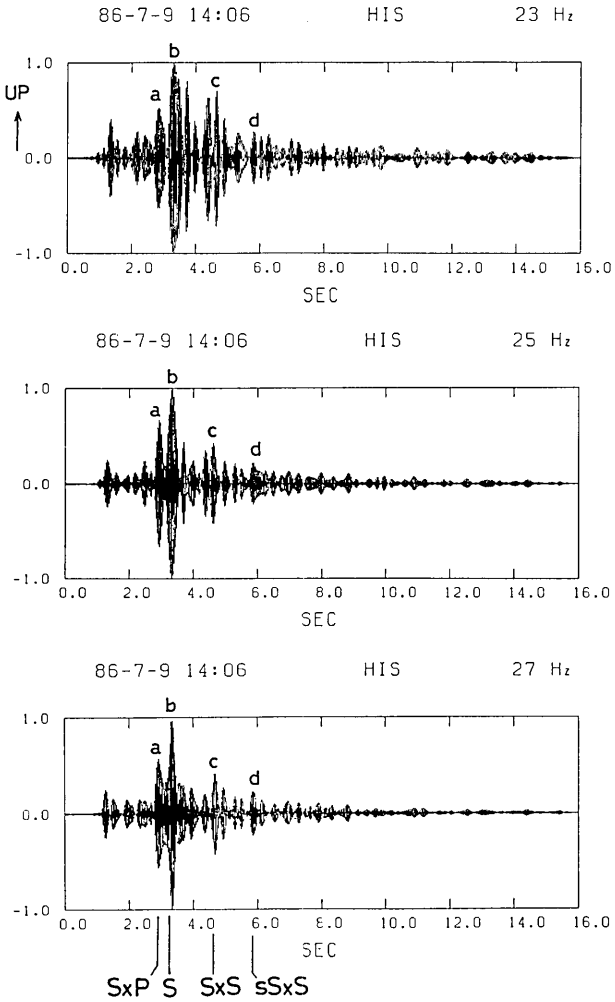

Fig. 14. Filtered seismograms through recursion digital filters without phase-delay for Event A shown in Fig. 10. The frequency bands are designed by $(0.909f, 1.1f)$, where f is the center frequency given in the figure. The frequency giving half of the amplitude is $1.2f$, i.e., the decay rate being 48.4 dB/oct. Interpreted reflected arrivals are indicated by their symbols.

4.2. Crustal Phases on Seismograms

The waveform from Event A in Fig. 10 is abundant in high frequency components at around the beginning of the S waves. By using narrow band-pass filters without phase delay we can more clearly recognize the appearance of such waves. Fig. 14 shows the filtered seismograms with several prominent wave packets. It should be noted that the marked phases are very stable for a slight shift of the frequency bands between 24 and 27 Hz compared with other neighboring ones. Since the most prominent wave is the direct S, it is quite natural to regard them as waves originating from an S wave. The 30 Hz-band filtered waveform shows a sharp phase around the direct P group and another clear phase between P and S arrivals (Fig. 15).

For the sake of simplicity we use the one-layer model shown in Fig. 16, and assume that the discontinuity surface is below the source, in order to explain all the phases at a time. A discontinuity above the source produces only one phase, or a P wave converted P from the S wave, other than direct P and S waves.

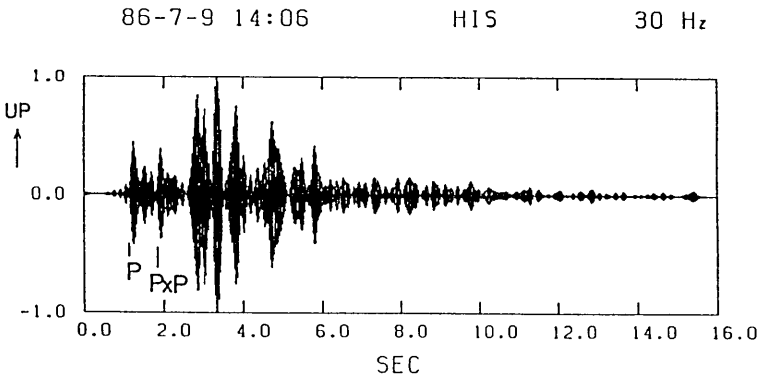

Fig. 15. Filtered seismogram of Event A for a 30 Hz band. Direct P and the corresponding PxP phases are identified.

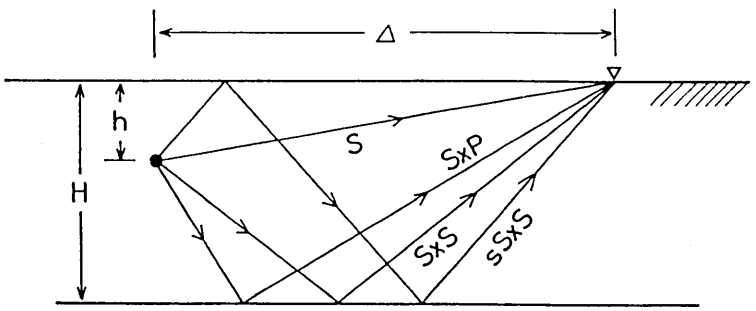

Fig. 16. Ray paths from a source to a station for various reflected waves.

The interpretation with only reflected waves from both the ground surface and an underground discontinuity is successful. The observed arrival time differences $T_{SxP}-T_S$, $T_{SxS}-T_S$ and $T_{sSxS}-T_S$ are -0.4 sec, 1.3 sec and 2.6 sec, respectively. Under the above constraints, we seek the optimum values of H, discontinuity depth, and h, focal depth, assuming that the P and S velocities of the layer are 6.0 km/s and 3.53 km/s. The result is summarized as follows: $H=8.9$ km and $h=3.1$ km with the standard deviation of the travel time residuals being 0.07 sec. The seismic wave velocities at shallow depths should be smaller than 6.0 km/s in V_p. If we assume V_p to be 5.8 km/s as suggested for the Adapazari region about 50 km northeast of our site from the seismic explosion study (GURBUZ *et al.*, 1980), leaving V_p/V_s unchanged, H and h are calculated to be 8.6 km and 3.0 km, respectively. On the other hand, the increase of V_p/V_s to 1.732 with V_p being 6.0 km/s brings the results of $H=8.8$ km and $h=3.0$ km. We can safely say that a discontinuity surface exists at around 8-9 km as far as our waveform interpretation is correct.

The unkown prominent phase just after the initial motion in Fig. 15 can be interpreted to be a PxP wave reflected at the discontinuity at $H=8.9$ km.

We can recognize two clear phases between P and S on the seismograms of the explosions recorded at GUN (Fig. 8). The source region is shown in Figs. 3 and 9. The first one is probably a reflected wave from a shallow 2 km deep discontinuity surface. The second could possibly be an SxP wave reflected at the depth of 8-9 km. This SxP is recognized on tne records at ALA for the same artificial events (Fig. 8). Taking account of the ray paths from both a natural microearthquake and artificial explosions, the discontinuity would exist at least in some part of the southern side of the Iznik-Mekece Fault.

5. Discussion

The eastern margin of the proposed seismicity gap is around the town of Adapazari, where the 1967 Mudurnu earthquake (M7.1) took place. The fault rupture along the North Anatolian Fault extends to some extent westward along the northern branch the Izmit-Sapanca Fault, whereas the southern branch, the Iznik-Mekece Fault, was not affected by that rupture (AMBRASEYS and ZATOPEK, 1969). However, the Iznik-Mekece Fault seems to be a smooth extension of the main fault from a topographic point of view. It is not certain that the high microseismic activity at the northern branching fault is related to the above nature. The highly active area seems to be limited to around Izmit City. There is, however, some possibility of swarm activity preceding an incoming large earthquake. That phenomon has been suggested by several authors (e. g. SEKIYA, 1976, KA-

NAMORI, 1983).

On the other hand, the western margin of the seismic gap is not so clear. The recent large earthquakes around the margin are the 1953 earthquake of $M7.2$ in the Yenice-Gonen area 100 km west of Bursa City, the 1964 event of $M6.6$ in Manyas near Bursa and the 1963 Cinarcik earthquake of $M6.2$ around the entrance of Izmit Bay, Marmara Sea (e.g. ERDIK, 1985). In the source region of the Cinarcik event, swarm-like activity has continued for a long time until the present thme (ÜÇER *et al.*, 1985).

Relatively recent historical large earthquakes that took place within the gap area are the 1878 earthquake whose source region is estimated to be between Izmit and Adapazari, and the 1894 event which is called the great lstandbul earthquake (AMBRASEYS, 1970). In 1897, a number of damaging earthquakes happened in the Yenisehir-Osmaneli-Bilecik area on the southern side of the Iznik-Mekece fault (AMBRASEYS and ZATOPEK, 1969).

The microseismic quiescence found by our observation in the vicinity of the Iznik-Mekece Fault may also suggest a possibility of the precursory phenomenon for a future big event as found often in seismicity in various regions (e.g. KELLEHER, 1970; WYSS and HARBERMANN, 1979). The low Q property is also possibly a precursor.

This region is situated in the eastern end of the large scale extensional tectonic field covering the wide area from Greece, through the Aegean Sea, to the western part of Anatolia. A number of focal mechanism solutions of this area show normal fault type with a tentional axis lying along roughly in the NNE-SSW direction (MCKENZIE, 1972). A recent plate tectonic interpretation on this situation is that the Aegean block of the Anatolian Micro-plate is rotating counter-clockwise against the eastern block due to side arc collision of plates near Crete, which would produce the extensional stress field (ROTSTEIN, 1985). In the gap region, the focal mechanisms of microearthquakes from the Izmit-Adapazari area show predominant normal fault solutions and the axis of tension in the same direction as found in the wide region (EVANS *et al.*, 1985). Beside this study, the TDP project (Turkish Dilatancy Project) (CRAMPIN *et al.*, 1985) revealed prevailing extended-dilatancy anisotropy (EDA) around the Izmit-Adapazari area, showing the existence of an extensional stress similar to the focal mechanism study (BOOTH *et al.*, 1985). The focal depths there are roughly between 8 and 10 km (EVANS *et al.*, 1985).

As mentioned above, this region is a special field where strike slip fault system and extensional tectonic features are combined together. In addition to this, there is some geological evidence to indicate a compressional stress regime near Sapanca Lake, along the Izmit-Sapanca fault, indicating the difference of tectonics between the shallow and the deep crust (IKEDA, 1988). The discontinuity surface at a depth of 8–9 km pro-

posed in this study may have something to do with this vertical separation of the crustal tectonic regime.

6. Conclusion

The nearly continuous observation during 39 days in the midst of the proposed seismicity gap revealed the extremely low seismicity in the vicinity of the Iznik-Mekece Fault, the southern branch of the North Anatolian Fault to the west. A probability consideration indicates that the microseismic rate is 23.0 events per year with a significance level of 10%. The high ability of detection of our observation system is evident from the fact that the microearthquake swarm including events of $M=0$ in a surrounding region, 25 km away from Alakaya station in the northern branch of the North Anatolian Fault, was clearly detected.

Coda Q values obtained from digitized waveforms recorded on the cassette tapes are very low, between 30 and 200, in the fault region at frequencies from 2 to 10 Hz, compared with the values, between 70 and 300, of the surrounding region. The relatively low coda Q at lower frequencies may suggest that the crust in the vicinity of the fault zone is either highly heterogeneous for waves with wavelengths of 350–1800 m or in an anomalous state of increased intrinsic attenuation preparing for a forthcoming large earthquake.

Band-pass filtered waveforms of a local microearthquake show predominant phases other than the usual P and S waves, at higher frequencies from 20 to 30 Hz. In terms of a simple crustal structure model with a horizontal discontinuity surface at some depth, we interprete those phases as arrivals reflected from the horizontal discontinuity at a depth of 8–9 km. This discontinuity, which is also interpreted to generate a reflected arrival on the seismograms of a series of explosions, may exist at least locally on the southern side of the Iznik-Mekece Fault. If this discontinuity exists extensively, it may provide a key to understanding the difference between a compressional stress regime for the shallow crust suggested by surface geology and a tentional one for the deep crust inferred from seismic studies. The authors recognize that this discontinuity hypothesis should be reexamined from more data and other aspects in a future study.

Acknowledgments

The authors are grateful to Prof. M. Dizer, Director of Kandilli Observatory and Earthquake Research Institute, Boğaziçi University, for his support to our work. The authors wish also to thank Mr. Doğan Kalafat, Mr. Nafiz Kafadar and Ms. S. Puskülcü at Kandilli Observatory for assist-

ing us in the observation and data handling works. Thanks are extended to Prof. Kazuo Oike of Kyoto University for his kind advice and help in preparing seismic instruments and Mr. Norio Hirano at Hokuriku Micro-earthquake Observatory, Kyoto University, for using his cassette tape data reproduction system. This study was supported partially by a Grant-in-Aid for International Scientific Research No. 61041029, Ministry of Education, Science and Culture, Japan.

References

AKI, K., 1980, Scattering and attenuation of shear waves in the lithosphere, *J. Geophys. Res.*, **85**, 6496-6504.

AMBRASEYS, N. N. and A. ZATOPEK, 1969, The Mudurnu valley, west Anatolia, Turkey, earthquake of 22 July 1967, *Bull. Seism. Soc. Am.*, **59**, 521-589.

AMBRASEYS, N. N., 1970, Some characteristic features of the Anatolian fault zone, *Tectonophysics*, **9**, 143-165.

BOOTH, D. C., S. CRAMPIN, R. EVANS and G. ROBERTS, 1985, Shear-wave polarizations near the North Anatolian Fault 1. Evidence for anisotropy-induced shear-wave splitting, *Geophys. J. R. Astr. Soc.*, **83**, 61-73.

CRAMPIN, S. and S. ÜÇER, 1975, The seismicity of the Marmara sea region of Turkey, *Geophys. J. R. asttr. Soc.*, **40**, 269-288.

CRAMPIN, S., R. EVANS and B. K. ATKINSON, 1984, Earthquake prediction: a new physical basis, *Geophys. J. R. Astr. Soc.*, **76**, 147-156.

CRAMPIN, S., R. EVANS and S. B. ÜÇER, 1985, Analysis of local earthquakes: the Turkish Dilatancy Projects (TDP1 and TDP2), *Geophys. J. R. Astr. Soc.*, **83**, 1-16.

ERDIK, M., V. DOYURAN, N. AKKAS and P. GULKAN, 1985, A probabilistic assessment of the seismic harzard in Turkey, *Tectonophysics*, **117**, 295-344.

EVANS, R., I. ASUDEH, S. CRAMPIN and S. B. ÜÇER, 1985, Tectonics of the Marmara sea region of Turkey: new evidence from micro-earthquake fault plane solutions, *Geophys. J. R. Astr. Soc.*, **83**, 47-60.

GÜRBÜZ, C., S. B. ÜÇER, H. ÖZDEMIR, 1980, Preliminary results of seismic refraction measurements using quarry blast in Adapazari region, *Deprem Arastirna Enst. Bulteri*, **31**, 73-88 (in Turkish).

IKEDA, Y., 1988, Geomorphological Observation of the North Anatolian Fault Zone, west of Mudurnu, *Multidiciplinary Research on Fault Activity in the Western Part of the North Anatolian Fault Zone*, (Eds., Y. HONKURA and A. M. IŞIKARA), 6-14.

JIN, A. and K. AKI, 1986, Temporal change in coda Q before the Tangshan earthquake of 1976 and the Haicheng earthquake of 1975, *J. Geophys. Res.*, **91**, 665-673.

KANAMORI, H., 1981, The nature of seismicity patterns before large earthquakes, *Earthquake Prediction—an international review, Maurice Ewing Series 4, American Geophysical Union*, 1-19.

KELLEHER, J. A., 1970, Space-time seismicity of the Alaska-Aluetian seismic zone, *J. Geophys. Res.*, **75**, 5745-5756.

LOWELL, J. H., S. CRAMPIN, R. EVANS, S. B. ÜÇER, 1987, Microearthquakes in the TDP swarm, Turkey: Clustering in space and time, *Geophys. J. R. Astr. Soc.*, **91**, 313-330.

MCKENZIE, D. P., 1972, Active tectonics of the Mediterranean region, *Geophys. J. R. Astr. Soc.*, **30**, 109-185.

MOGI, K., 1979, Two kinds of seismic gaps, *Pure Appl. Geophys.*, **117**, 1172-1186.

OIKE, K. and K. MATSUMURA, 1985, A new recording system of seismic waves using audio recorder, *Zisin*, **38**, 359-364 (in Japanese).

ROTSTEIN, Y., 1985, Tectonics of the Aegean block: Rotation, side arc collision and crustal extension, *Tectonophysics*, **117**, 117-137.

SEKIYA, H., 1976, The seismicity preceding earthquakes and its significance to earthquake prediction, *Zisin*, **29**, 299-311 (in Japanese).

SIPAHIOĞLU, S. and T. MATSUDA, 1986, Geology and Quaternary fault in the Iznik-Mekece area, *Electric and Magnetic Research on Active Faults in the North Anatolian Fault Zone*, (Eds., A. M. ISIKARA and Y. HONKURA), 25-41.

TOKSÖZ, M. N., A. F. SHAKAL and A. J. MICHAEL, 1979, Space-time migration of earthquakes along the North Anatolian Fault Zone and seismic gaps, *Pure Appl. Geophys.*, **117**, 1258-1270.

TSUKUDA, T., 1988, Coda-Q before and after the 1983 Misasa earthquake of M6.2, Tottori Prefecture, Japan, *Pure Appl. Geophys.*, **128**, 261-279.

ÜÇER, S. B., S. CRAMPIN, R. EVANS and N. KAFADAR, 1985, The MARNET radio linked seismometer network spanning the Marmara sea and the seismicity of western Turkey, *Geophys. J. R. Astr. Soc.*, **83**, 17-30.

WYSS, M. and R. E. HABERMANN, 1979, Seismic quiescence precursory to a past and a future Kurilles islands earthquake, *Pure Appl. Geophys.*, **117**, 1195-1211.

トルコ北アナトリア断層帯，イズニック・メケジェ断層付近における低い地震活動や低いコーダ Q 値，上部地殻の不連続面について

地震研究所　佃　為成

東京工業大学理学部　佐竹健治，本蔵義守

Kandilli Observatory, Boğaziçi University　S. Balamir ÜÇER, A. Mete IŞIKARA

北アナトリア断層帯西部の地震空白域，イズニック・メケジェ断層付近において，1986年7月6日から8月13日の間，はじめての高感度地震観測を実施した．地震計は固有周波数 2 Hz の上下動成分のみを使用し，6ケ所に観測点を設けた．3点には可視記録方式，あとの3点にはアナグロのカセットテープの記録計を用いた．11個の電源が決められたが，これらはいずれも当該断層から数10 km 離れている．震源が決まらなかった断層付近の微小地震は4回であった．統計的には10%の危険率で23回/年の微小地震が発生すると言える．カセットテープに記録された数少ない地震の波形を解析し，断層付近でコーダ Q が低いことや，その直下，深さ 8～9 km 付近に地震速度の不連続面が存在することが反射波の解釈から推定された．これらの性質はその地域の地震予知やテクトニクスの問題にも関わっている．